The role of mono-atomic steps and of step decoration by Cu on the adsorption and hydrogenation of benzene and cyclohexene on Pt single crystal electrodes

5 AUTHORS, INCLUDING:

Pavel Janderka
Pragolab Ltd.

22 PUBLICATIONS   **46** CITATIONS

SEE PROFILE

Helmut Baltruschat
University of Bonn

156 PUBLICATIONS   **2,557** CITATIONS

SEE PROFILE

The role of mono-atomic steps and of step decoration by Cu on the adsorption and hydrogenation of benzene and cyclohexene on Pt single crystal electrodes

Th. Löffler [a], R. Bussar [a], E. Drbalkova [b], P. Janderka [b], H. Baltruschat [a],*

[a] *Institut für Physikalische und Theoretische Chemie, Universität Bonn, Römerstrasse 164, D-53117 Bonn, Germany*
[b] *Institut Theoretical and Physical Chemistry, Faculty of Science, Masaryk University, Kotlarska 2, CZ-61137 Brno, Czech Republic*

Abstract

The adsorption of benzene and cyclohexene was studied at the stepped $Pt(332) = Pt(s)[6(111) \times (111)]$ and at the $Pt(111)$ electrode surface using differential electrochemical mass spectrometry (DEMS). The experiments involve desorption and hydrogenation in the hydrogen region, oxidation in the oxygen adsorption region and non-reactive displacement by underpotential deposition of Cu. The results are compared with those obtained previously at $Pt(111)$ and at $Pt(110)$. The total coverage is similar on all surfaces and for both molecules ($0.3–0.4$ nmol cm^{-2}). Benzene adsorbed at the $Pt(332)$ electrode desorbs nearly quantitatively as cyclohexane during potential sweeps to the hydrogen region below 0.05 V, similar to the case of the $Pt(110)$, whereas benzene is desorbed without hydrogenation from $Pt(111)$ below 0.2 V. Therefore, the step density of the $Pt(332)$ is sufficiently large or the ratio of the terrace width to the size of the molecule is small enough so that a larger number of the molecules are influenced by the steps and are hydrogenated. Decoration of the steps by Cu previous to adsorption of benzene or cyclohexene reduces the adsorbate coverage by a factor of 2, although only around 20% of all adsorption sites are blocked by Cu. This shows, that the rows of Cu are a hindrance for a dense adlayer of the adsorbate. Hydrogenation of the adsorbate is largely diminished, proving that the step sites are the catalytic sites for the hydrogenation reaction. Whereas previous experiments on the displacement of the adsorbate on $Pt(110)$ by UPD of Cu had shown that cyclohexene is dehydrogenated to benzene upon adsorption, similar experiments on $Pt(111)$ show that less than one third of the total adsorbate (0.08 nmol cm^{-2}) are displaced as cyclohexene. Only one tenth of the adsorption product of cyclohexene on $Pt(332)$ is displaceable, solely as benzene, under these non-reactive conditions. Therefore, dehydrogenation is also only occurring at the step sites, but adsorption leading to another, more abundant adsorption product, which is not displaceable, seems to be faster.
© 2003 Elsevier Ltd. All rights reserved.

Keywords: Adsorption; Hydrogenation; Benzene; Electrocatalysis; DEMS

1. Introduction

Fundamental understanding of the adsorption and desorption reactions of unsaturated hydrocarbons is of great interest for both electrochemists and surface scientists. The adsorption of benzene and cyclohexene on platinum single crystals has been intensively studied in the past at the gas–solid interface [1–6]. One aim of these studies was to examine the catalytic properties of steps concerning the dehydrogenation of cyclohexene (forming benzene) and the hydrogenation of benzene. Muetterties et al. showed that the stepped platinum surface of the Pt(332) is more active for cyclohexene conversion to benzene than the flat Pt(111) surface [6]. At 25 °C they could not detect any benzene, i.e. no dehydrogenation of adsorbed cyclohexene, on Pt(111), based on the displacement by trimethylphosphine after adsorption of cyclohexene. In contrast, the stepped surface (Pt(332)) converted cyclohexene to chemisorbed benzene at this temperature.

In the recent years all studies in UHV were focused on the adsorption of benzene and cyclohexene on the low index surfaces Pt(111) [7–10], Pt(100) [10] and Pt(110) [11–13], completely disregarding the influence of step

* Corresponding author. Fax: +49-228-73-4540.
E-mail address: baltruschat@uni-bonn.de (H. Baltruschat).

density on the dehydrogenation and hydrogenation of these adsorbed model species. The work was more or less focused on the adsorption geometry and the intermediates formed during the surface reactions of the adsorbed C_6-species.

Besides this experimental research the theoretical modeling of the C_6/Pt(111) system became of increasing importance. Neurock et al. analyzed the adsorption of benzene on Pt(111) using first-principles density functional theoretical cluster and periodic slab calculations [14]. The authors calculated that the preferred adsorption site at low coverage is the bridge site. The molecule's second important site is the hollow site, which becomes preferred at higher coverages.

As the solid–liquid interface is much less accessible, there is only a small number of methods that can be used to study adsorbate reactions of the above mentioned hydrocarbons at all. On the other hand, organic adsorbates on electrode surfaces and their surface reactions are of great importance for industrial processes under environmental conditions, e.g. for corrosion inhibition, as brighteners, as unwanted contents in fuels. Itaya and coworkers studied the adsorption of benzene on Pt(111) and Rh(111) in benzene containing solution using EC-STM [15]. They found ordered adlayers of adsorbed benzene with a c($2\sqrt{3} \times 3$)-rect-$2C_6H_6$) symmetry on both surfaces in the double-layer charging region. Xiao recently used EC-STM to study the benzene adsorption at Pt(111) in benzene free solution [16] and found the same structure.

We have shown in the past that differential electrochemical mass spectrometry (DEMS) is well suited to investigate the influence of the surface structure on the adsorption and desorption reactions of hydrocarbons under electrochemical conditions [17]. In the case of adsorbed benzene it was shown, that the smooth Pt(111) and Pt(100) surfaces are inactive for hydrogenation to form cathodically cyclohexane, whereas in the case of the open Pt(110) and at Ptpc almost all adsorbate is hydrogenated to cyclohexane [18]. The direct oxidation of cyclohexene and benzene preadsorbed on these surfaces leads to complete oxidative desorption yielding only CO_2. In the case of benzene adsorbed at Pt(111) the formation of a benzoquinone-species as intermediate during the direct oxidation was postulated [19]. When adsorbing cyclohexene on Pt(110) and Ptpc, the adsorbate formed can be displaced at the adsorption potential by Cu-UPD, benzene being the sole product [20]. A comparison to the displacement of adsorbed benzene at these surfaces [21] clearly shows, that cyclohexene is dehydrogenated to benzene on these open surfaces.

Here we extend our study on the desorption of adsorbed cyclohexene and benzene at Pt(332) and show that steps are electrocatalytic sites for hydrogenation and dehydrogenation. Together with a study on ethene adsorption on Pt single crystal surfaces [22] the results suggest that the ratio of the terrace width to the size of the adsorbate determines the extent of hydrogenation.

It has been shown in the past that the step decoration with a second metal offers a unique possibility for studying ordered bimetallic surfaces and allows to gain informations on the catalytic action of the second metallic component [23–26]. This approach will be used here to study the geometric effect of a Cu modified surface on benzene adsorption.

2. Experimental

As electrochemical cell the one compartment thin layer cell was used, which is described in detail elsewhere [17]. The reaction products diffuse through a thin layer of electrolyte (50–100 μm) to a Teflon membrane, which separates the liquid phase from the gas phase of the differentially pumped mass spectrometer. Further details of the principle setup of the differentially pumped vacuum system are described in [17]. With an approximate delay of 2 s after the formation at the electrode surface (due to diffusion), the volatile species evaporate through the porous Teflon membrane and are detected mass spectrometrically. The mass spectrometer used were a Balzers QMG 511 or a QMG 422. Using the QMG 511 up to five different ion currents of possible desorption products can be recorded simultaneously to the cyclic voltammogramm. In the case of the QMG 422 up to 64 different ion currents can be measured. Usually, five different ion currents are sufficient for the identification of the possible desorption products.

The single crystal electrodes were prepared by annealing in a hydrogen flame, cooling down in a strong Ar stream and immersing in supporting electrolyte (always 0.5 M H_2SO_4). After checking the quality of the single crystal surface by cyclic voltammetry in a glass cell, the electrode was transferred into the thin-layer cell. During the whole transfer (ca. 1 min) the electrode surface was protected by a droplet of Ar saturated electrolyte. Afterwards cleanliness and surface quality was furthermore controlled by cyclic voltammetry. The adsorption process is performed by flushing ca. 1 ml of 0.5 M H_2SO_4 saturated with benzene or cyclohexene through the thin-layer cell for ca. 1 min. During the whole adsorption time (4 min) the potential was held at a value between 0.35 and 0.4 V versus RHE. After thorough electrolyte change with pure supporting electrolyte only benzene or cyclohexene adsorbed at the electrode remained in the thin-layer cell. This was controlled by measuring the ion current of m/z = 78 (benzene) or m/z 82 (cyclohexene) during the whole adsorption procedure. After adsorption, the potential was either swept in anodic ('direct oxidation') or cathodic direction ('cathodic desorption') under stopped flow of electrolyte. In the

case of the displacement experiments the copper containing electrolyte, 10^{-4} Cu^{2+} in 0.5 M H_2SO_4, was flushed through the one compartment thin-layer cell still at the adsorption potential with a constant flow rate of ca. 0.2–0.5 μl s^{-1}. After displacement, a complete electrolyte exchange with supporting electrolyte was performed.

All ion currents i shown here are normalized by division through the relative abundance of the fragment H_i, i.e. the relative contribution of a particular ion to the sum of the ion intensities of a given species, and, in the case of m/z = 44 (CO_2), divided by the number of C-atoms of the respective molecule. To determine the surface concentration of an adsorbate via the amount of desorbing species, the mass spectrometer has to be calibrated under similar conditions as in the desorption experiments, i.e. similar flux of molecules and simultaneously evaporation of water in the vacuum. The calibration constant K* for CO_2 can be calculated from the faradaic charge and the ion charge of CO_2 from the electrochemically oxidation of adsorbed CO. Please note that the non-faradaic charge caused by different double layer charging at the free and the CO covered surface has to be subtracted. The amount of this non-faradaic part is ca. 20% of the oxidation charge on Pt [27]. In the case of other substances the calibration can be performed by dosing them into the mass spectrometer via a leak valve. The calibration is described in detail elsewhere [17] and was repeated for CO_2 and at least one other substance after each assembling of the thin-layer cell and electrode. Please note that the transfer efficiency N under stopped flow is close to 100%, whereas in the case of the displacement experiments, where a small flow through has to be used in order to introduce the Cu into the cell, N is even at such low flow rates of ca. 0.2 μl s^{-1} not well defined and amounts to ca. 0.5. The base levels of mass signals were subtracted from the ion currents before integrating the signals. The procedure to obtain the quantities of desorbed products and thus the surface concentration Γ is also described in [17]. The geometric surface area of the working electrode is given by the inner diameter of the Teflon spacer in the thin layer cell. This value was always compared with the real surface area as determined from the hydrogen adsorption/desorption charge of the bare electrode in the thin layer cell. In some cases the experimental value of the real surface area exceeds the nominal geometric surface area due to high flexibility of the spacer. Therefore, in all cases the real surface area was used for the calculation of the surface concentration Γ. The number of electrons n_{ox}, which is released when one adsorbed molecule is oxidized to CO_2, can be determined from the ratio of the faradaic charge (Q_f) to the ion charge (Q_i) (of m/z = 44) multiplied with the calibration constant K* for CO_2 and the number of C-atoms of the respective molecule [19]. The

Q_f values for the oxidation were determined by integration over three whole potential cycles, using the charge of the fourth cycle as background, since all adsorbed species were oxidatively removed within three anodic cycles. Contrary, to the case of CO oxidation, where approximately 20% have to be subtracted from the oxidation charge, the charge for the oxidation of aromatic molecules is much larger and double layer charging should be negligible. The calculated values (n_{ox} and Γ) were reproducible to within ±15%.

3. Results

3.1. Direct oxidation

Fig. 1 shows the CV-curves and the corresponding mass spectrometric cyclic voltammogramms (MSCV) for m/z 44 (CO_2) during direct oxidation of preadsorbed benzene and cyclohexene on Pt(332). The adsorbed benzene is completely removed within three anodic cycles, as in the case of Pt(111), Pt(100), Pt(110) and Ptpc [18,19]. In the case of benzene two oxidation waves are visible in the CV; the first (at 0.88 V) does not yield CO_2 as oxidation product, as already observed before on Pt(111) [19]. There benzoquinone was assumed to be the partially oxidized species formed as an intermediate.
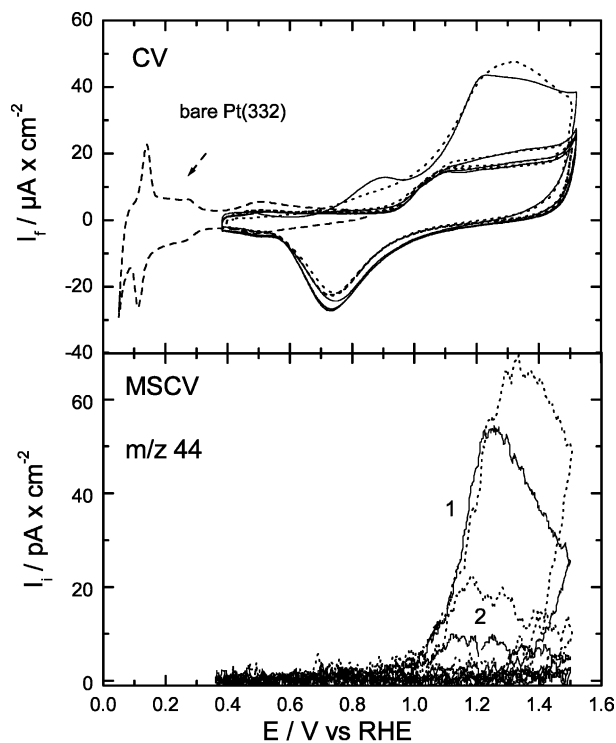

Fig. 1. Direct oxidation of preadsorbed benzene (solid line) and cyclohexene (dotted line) at Pt(332); $E_{ad} = 0.4$ V, v = 10 mV s^{-1}, 0.5 M H_2SO_4. Top: CV (dashed line: bare Pt(332) in supporting electrolyte: 20 mV s^{-1}, the current is divided by a factor of 2). Bottom: MSCV: m/z = 44: CO_2; the numbers indicate the number of the cycle.

The second oxidation wave is accompanied by the formation of CO_2 (onset above 0.9 V) with a maximum at 1.23 V. When adsorbed cyclohexene is directly oxidized (Fig. 1) one also can distinguish two oxidation waves. The first oxidation wave again occurs without formation of CO_2, but is only a shoulder in the CV curve 0.88 V. The maximum of the second oxidation step is shifted to 1.3 V. The MSCV shows that the formation of CO_2 also starts above 0.9 V. The number of electrons n_{ox} transferred per oxidized cyclohexene is 34 similar to the n_{ox} value for adsorbed benzene at Pt(332), which amounts to 35. In the case of cyclohexene on Ptpc, Pt(111) or Pt(110) [28] we determined n_{ox} values between 39 and 42. In the case of benzene adsorbed on Pt(111) [29] the n_{ox} was 40 and in the case of the Ptpc 37. The corresponding theoretical values are 34 and 30, respectively. Due to the experimental error of theses values ($\pm$ 15%), however, they do not allow to determine the exact identify of the species unequivocally.

The total surface concentrations Γ calculated from the ion charges of m/z = 44 (CO_2) are within the error of $\pm 15\%$ in good agreement with the results obtained for the other monocrystalline surfaces.

3.2. Cathodic desorption

Fig. 2 shows the CV and MSCV curves of the cathodic desorption of adsorbed benzene at Pt(332) and the subsequent oxidation of the remaining adsorbate. The CV curve shows that the desorption from terrace sites during the first cathodic sweep is nearly complete, since the suppression of the corresponding hydrogen adsorption [32] is lifted in the following anodic sweep. The peak due to adsorption/desorption of hydrogen at the steps (0.12 V) increases to some extend with further sweeps (up to the fourth cycle), indicating that little desorption from the steps still continues. The corresponding MSCV shows that benzene (m/z = 78) desorption starts below 200 mV only during the first cathodic sweep. The onset (50 mV) of cyclohexane formation (m/z = 84) coincides with the decrease of the benzene signal, as shown before for Pt(111) [19]. Please note that we have shown in the past that no reaction between H_2 and benzene occurs in the mass spectrometer [33]. Contrary to benzene, cyclohexane is also desorbed in the second sweep. This, together with the observation from the CV, allows the assumption, that species adsorbed at step sites desorb as cyclohexane. No partially hydrogenated products were detected, as no signals were observed for m/z = 80 and 82. When increasing the upper potential limit to 1.5 V the remaining adsorbate is completely oxidized solely to CO_2 within three cycles.

In order to examine whether the relative amount of hydrogenation is thermodynamically or kinetically controlled, we performed a potential stop experiment.
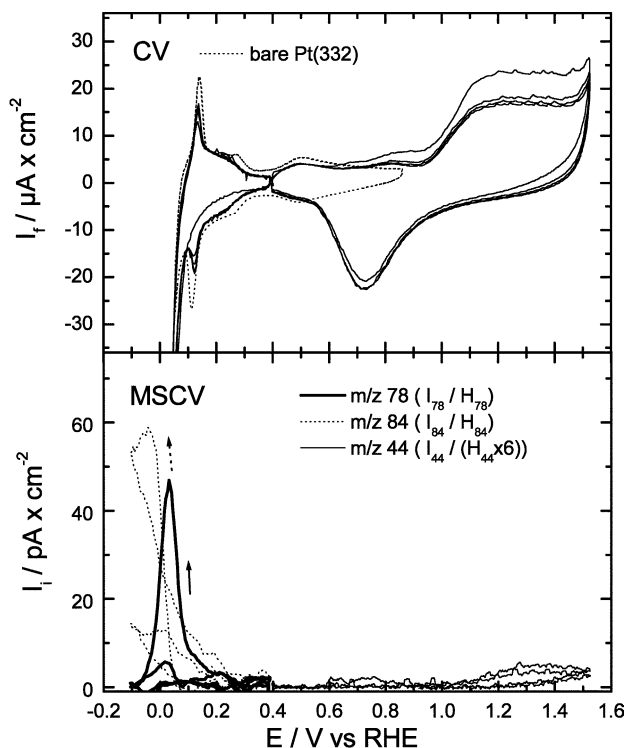

Fig. 2. Cathodic desorption of preadsorbed benzene at Pt(332) (four cycles between 0.4 and −0.1 V) and subsequent oxidation of the remaining adsorbate; please note that the large cathodic faradaic currents are cut off due to an expansion of the current scale $E_{ad} = 0.4$ V, v = 10 mV s^{-1}, 0.5 M H_2SO_4. Top: CV (dashed line: bare Pt(332) in supporting electrolyte: 20 mV s^{-1}, the current is divided by a factor of 2). Bottom: MSCV: solid line (thick) m/z = 78: benzene; dotted line m/z = 84: cyclohexane; solid line (thin) m/z = 44: CO_2.

When the potential is stopped for 5 min within the first cathodic sweep during cathodic desorption of adsorbed benzene at Pt(332) at 70 mV only benzene desorbs (not shown here). In the subsequent sweep further in cathodic direction cyclohexane desorbs below 0.05 V and only traces of benzene can be detected. During the second sweep no desorption of benzene, but further formation of cyclohexane below 0.05 V is observed, identically to the desorption experiments without potential stop. Again the further formation of cyclohexane coincides in the CV with an increase of the hydrogen adsorption/desorption charge at the step sites only, whereas the charge of the hydrogen adsorption/desorption at the terrace stays constant after the first cathodic cycle, identically to the desorption experiment without potential stop. The subsequent anodic oxidation of the remaining adsorbate is similar to the desorption experiment without potential stop.

In order to prove that steps are electrocatalytic sites for the hydrogenation of adsorbed unsaturated organics, we examined the desorption of benzene adsorbed at a Pt(332) surface the steps of which had been decorated with Cu. The cathodic desorption of benzene adsorbed at Pt(332) with steps decorated by Cu-UPD is shown in

Fig. 3. Again, benzene desorption (< 0.2 V) can be observed only in the first cathodic sweep, whereas the formation of cyclohexane (ca. 50 mV) is visible also in the second cathodic cycle. The ratio of the amounts of desorbing cyclohexane to benzene is about 1:2, whereas in the case of the unmodified Pt(332) a ratio of about 5:1 was obtained (Fig. 2). Therefore, the catalytic activity for the hydrogenation of the Pt(332) surface has been drastically reduced by blocking the steps with the inactive Cu. In the case of Pt(111) the ratio of desorbing cyclohexane to benzene even amounts to 1:7 [19]. The remaining hydrogen adsorption/desorption charge at 0.12 V in the CV of the step decorated Pt(332) (see inset Fig. 3) therefore suggests that not all step sites had been blocked by Cu. From the ratio of the hydrogen adsorption charges (peak at 0.12 V) after copper deposition to that of the bare surface one can estimate that roughly 5% of the step sites had not been decorated. This is certainly the reason for the higher amount of cyclohexane than in the case of the Pt(111). The remaining adsorbate and the Cu-UPD (peak at 0.66) is
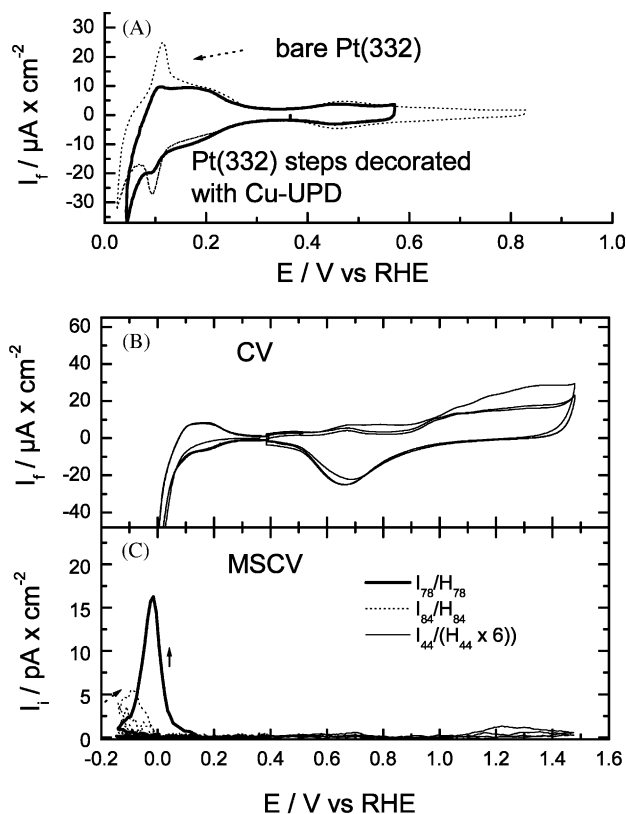
oxidized in the subsequent anodic oxidation cycles up to 1.5 V. The MSCV curve is similar to those shown before for the unmodified Pt(332).

The cathodic desorption with subsequent oxidation of cyclohexene adsorbed on Pt(332) (shown in Fig. 4) is, with respect to the shape of the CV and the MSCV curves and the on-set potentials, nearly identical to the case of adsorbed benzene. Differently from the Pt(111) surface, no desorption of cyclohexene can be detected. The ratio of desorbing cyclohexane to benzene is in the case of adsorbed cyclohexene on Pt(332) about 11:1, and therefore more than two times higher compared with benzene adsorbed at Pt(332).

Again, we performed adsorption/desorption experiments at step decorated Pt(332) electrode. The cathodic desorption of the adsorbate formed from cyclohexene adsorbed on Pt(332) with steps decorated by Cu-UPD is shown in Fig. 5. During cathodic sweeps benzene and only traces of cyclohexane (not shown) can be detected. Furthermore a signal on mass 82 can be observed, indicating the desorption of cyclohexene. The same species could be detected in the case of a Pt(111)-surface [30], clearly showing that the step decorated Pt(332) behaves similar to Pt(111). In the subsequent anodic
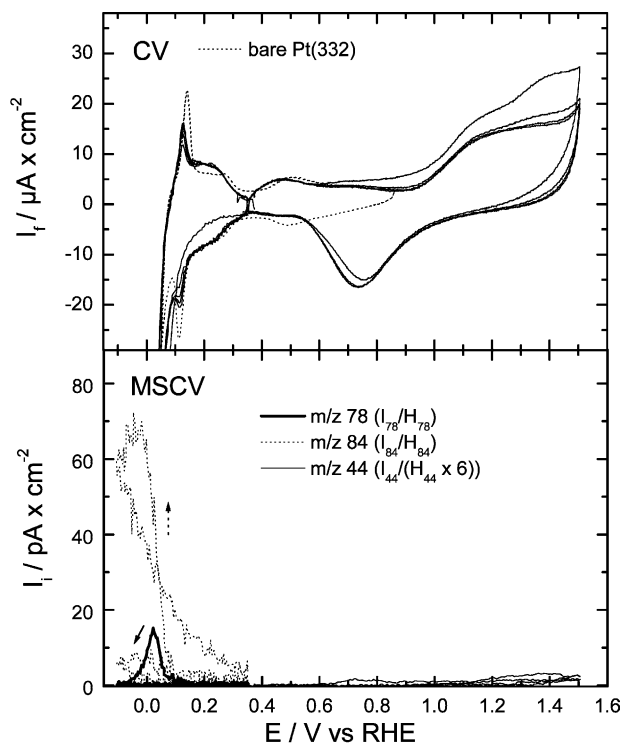

Fig. 3. Cathodic desorption of preadsorbed benzene at Pt(332) with the steps decorated by Cu-UPD (four cycles between 0.4 and −0.12 V) and subsequent oxidation of the remaining adsorbate; please note that the large cathodic faradaic currents are cut off due to an expansion of the current scale $E_{ad} = 0.36$ V, $v = 10$ mV s^{-1}, 0.5 M H$_2$SO$_4$. (A) Dotted line: bare Pt(332) in supporting electrolyte; solid line: step decorated Pt (332) in supporting electrolyte. (B) CV. (C) MSCV: solid line (thick) m/z = 78: benzene; dotted line m/z = 84: cyclohexane; solid line (thin) m/z = 44: CO$_2$.

Fig. 4. Cathodic desorption of preadsorbed cyclohexene at Pt(332) (four cycles between 0.4 and −0.1 V) and subsequent oxidation of the remaining adsorbate; please note that the large cathodic faradaic currents are cut off due to an expansion of the current scale $E_{ad} = 0.35$ V, $v = 10$ mV s^{-1}, 0.5 M H$_2$SO$_4$. Top: CV (dashed line: bare Pt(332) in supporting electrolyte: 20 mV s^{-1}, the current is divided by a factor of 2). Bottom: MSCV: solid line (thick) m/z = 78: benzene; dotted line m/z = 84: cyclohexane; solid line (thin) m/z = 44: CO$_2$.
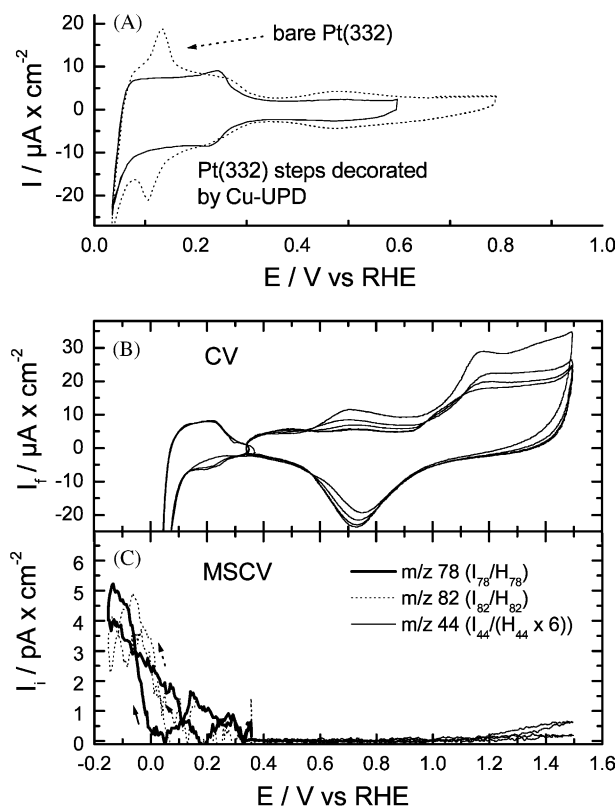
Fig. 5. Cathodic desorption of preadsorbed cyclohexene at Pt(332) with the steps decorated by Cu-UPD (four cycles between 0.4 and −0.12 V) and subsequent oxidation of the remaining adsorbate; please note that the large cathodic faradaic currents are cut off due to an expansion of the current scale $E_{ad} = 0.36$ V, v = 10 mV s^{-1}, 0.5 M H$_2$SO$_4$. (A) Dotted line: bare Pt(332) in supporting electrolyte solid line: step decorated Pt (332) in supporting electrolyte. (B) CV. (C) MSCV: solid line (thick) m/z = 78: benzene; dotted line m/z = 82: cyclohexene; solid line (thin) m/z = 44: CO$_2$.

cycles up to 1.5 V the Cu-UPD, peak at 0.7 V, and the remaining adsorbate is completely oxidatively removed (as CO$_2$) within three sweeps. The peak at 1.15 V due to oxygen adsorption at step sites [22,34] is more pronounced in this experiment than in Fig. 3, because due to decoration of steps with Cu no organic is adsorbed at step sites which might hinder oxygen adsorption.

3.3. Displacement of adsorbed cyclohexene at Pt(111) and Pt(332) by Cu-UPD

The comparison of the MSCV curves in Fig. 4 with the corresponding ones for benzene (Fig. 2) shows, that the adsorbate formed from cyclohexene at Pt(332) behaves similar to adsorbed benzene. Therefore, the non-reactive displacement with Cu-UPD of cyclohexene adsorbed at Pt(111) and at Pt(332) should identify the adsorbed species and show whether the stepped surface is active for the dehydrogenation upon adsorption.

When introducing copper containing solution into the cell after cyclohexene adsorption at Pt(111) (still at the

adsorption potential), a signal for m/z = 82 (inset Fig. 6) but not for m/z = 78, 80 and 84 (not shown here), which were simultaneously recorded, can be observed. Therefore, only cyclohexene desorbs during Cu adsorption. Fig. 6 shows the subsequent oxidation of the remaining adsorbate. In the CV two oxidation waves can be observed. The first with a maximum at 0.73 V involves the oxidation and desorption of copper. The second wave has a broad maximum at 1.38 V due to the oxidation of the remaining adsorbate to CO$_2$ as revealed by the MSCV. In the following cycles, Cu is readsorbed and desorbed again, but the size of the peak decreases due to some residual flow of electrolyte leading to a loss of Cu from the corresponding thin layer volume and is shifted to 0.6 V.

During the displacement experiment performed with cyclohexene adsorbed at Pt(332) only a signal for m/z 78 and no signals for m/z 80, 82 and 84 can be detected (not shown here). Therefore, only benzene desorbs during Cu adsorption. Fig. 7 shows the subsequent oxidation cycles direct after the displacement. In the CV two oxidation waves can be observed. The first with a maximum at 0.78 V again involves the oxidation of Cu-UPD paralleled by the oxidation of the remaining adsorbate. The MSCV curve shows, that formation of CO$_2$ starts
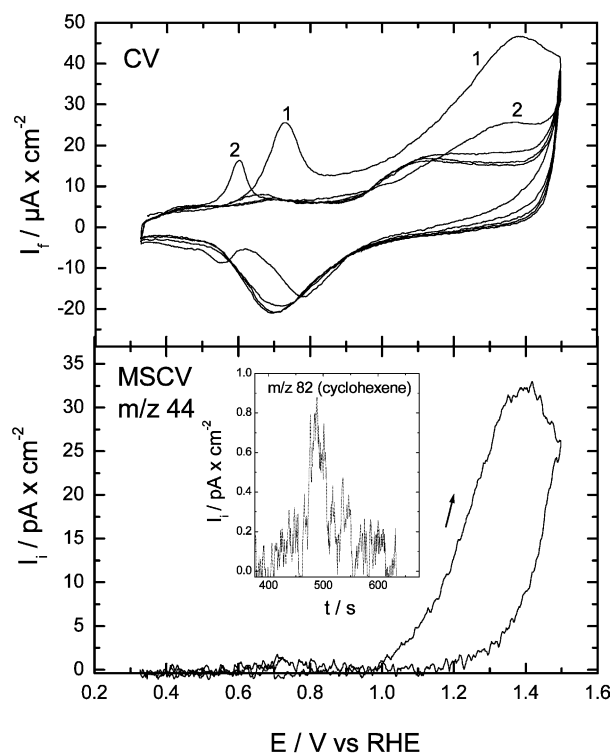

Fig. 6. Cyclohexene adsorption on Pt(111): displacement by Cu-UPD $E_{ad} = 0.35$ V, v = 10 mV s^{-1}, 0.5 M H$_2$SO$_4$. Top: CV: Oxidation of the adsorbate, which is not displaced by Cu-UPD. The numbers indicate the number of the cycle. bottom: MSCV: inset: ion current transient for m/z = 82 (cyclohexene); the arrow indicates the start of the displacement experiment m/z = 44: CO$_2$.
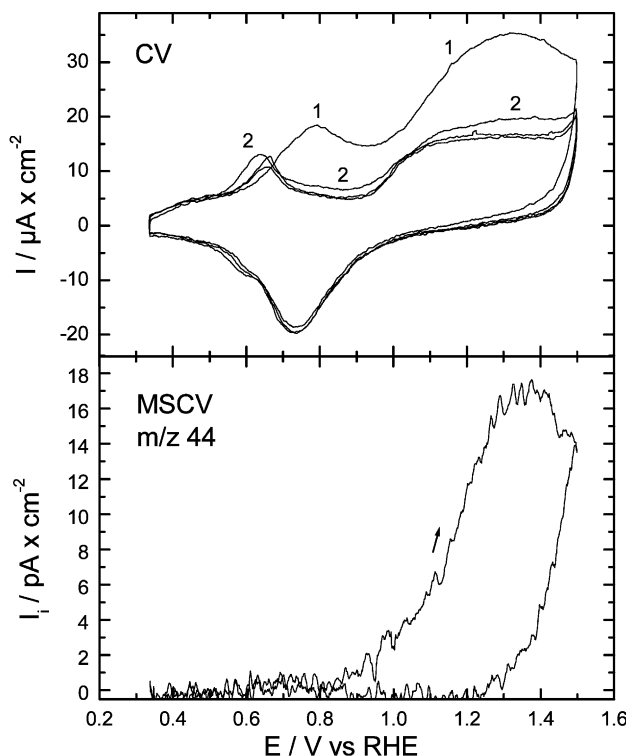
Fig. 7. Cyclohexene adsorption on Pt(332): displacement by Cu-UPD $E_{ad} = 0.35$ V, v = 10 mV s^{-1}, 0.5 M H$_2$SO$_4$. Top: CV: Oxidation of the adsorbate, which is not displaced by Cu-UPD. The numbers indicate the number of the cycle bottom: MSCV: m/z = 44: CO$_2$.

above 0.8 V. The second wave has a maximum at 1.35 V. Again some copper remains in the thin-layer (second sweep: peak at 0.64 V), the amount of which decreases from sweep-to-sweep.

4. Discussion

The quantitative results of desorption and displacement of adsorbed benzene and cyclohexene are summarized in Fig. 8 together with previous results [18–20,35]. The total surface concentrations are (within the experimental error of $\pm 15\%$) identical to those determined from the direct oxidation experiments (see Table 1).

4.1. Oxidation processes at the stepped surface

As already shown before for Pt(111) [19], also on Pt(332) adsorbed benzene is first oxidized to an adsorbed intermediate without formation of CO$_2$. Also here we assume that adsorbed benzoquinone is formed. Since this surface reaction is very structure sensitive—it was neither observed on Pt(110), Pt(100) nor on polycrystalline Pt [18]—we have to assume that it is due to benzene adsorbed at terrace sites.

In the case of the direct oxidation of cyclohexene adsorbed at Pt(332) the corresponding first oxidation wave is reduced to a shoulder. This indicates that some but not a large part of cyclohexene may be converted to adsorbed benzene on this surface.

4.2. Steps as catalytic sites for hydrogenation

In both cases, adsorbed benzene or cyclohexene at Pt(332), ca. 80% of the adsorbate can be desorbed cathodically mostly as cyclohexane and only to a small extent as benzene. This is similar to Ptpc or Pt(110) and completely different from Pt(111). It is obvious that the step density of the Pt(332) surface is sufficient for more or less complete hydrogenation of the adsorbed C$_6$-species presented here. In the case of ethene adsorbed on Pt(332) about 50% [22] and in the case of Pt(110) about 80% [20] of the adsorbed species can be desorbed under hydrogenative conditions. This suggests that the ratio of the terrace width to the size of the adsorbed molecule plays an important role for the hydrogenation efficiency.

Rodriguez and Pastor recently reported that during the cathodic desorption of benzene adsorbed on porous Ptpc cyclohexene is formed, as they detected a signal for m/z = 67 [36], the most intense (100%) peak of cyclohexene. Nevertheless, the authors did not take into account the relative abundance H_{67} of the mass fragment m/z = 67 of cyclohexane. In the case of cyclohexane the ratio of the mass fragment of m/z = 67 ($H_{67} \approx 0.009$) to m/z = 84 ($H_{84} \approx 0.15$) amounts to ca. 0.06. Since we did not find any indication for a desorption of cyclohexene on Pt(332) and also had not found any on Pt(110) [18], recording the ion intensity on m/z = 82, we recently reexamined the cathodic desorption of benzene adsorbed on porous Ptpc [37]. These results clearly show that the intensity on m/z = 67 is only due to fragmentation of cyclohexane and not due to the formation of cyclohexene, as the ratio of the ion charges of m/z = 67 and m/z = 84 is 0.05 and no ion current is observed for m/z = 82. Please note that for cyclohexene H_{82}/H_{67} is 0.35 and therefore the formation of cyclohexene should be clearly (and uniquely) observable at m/z = 82.

When the steps of the Pt(332) surface are decorated by electrocatalytically inactive Cu-UPD, the ratio between desorbing benzene and cyclohexane during cathodic desorption of adsorbed benzene is inverted. The desorption of benzene becomes predominating, as at Pt(111) [18]. The corresponding experiments with cyclohexene adsorbed on Pt(332) and on Pt(332)/Cu also show that the step decorated Pt(332) surface behaves like a Pt(111) surface. These findings are a clear evidence for the steps being electrocatalytic sites for the hydrogenation.

What determines the ratio of the amount of cyclohexane formed to that of benzene? One possibility is that it depends on the adsorption site, e.g. the distance to the step sites, whether an adsorbed benzene molecule is
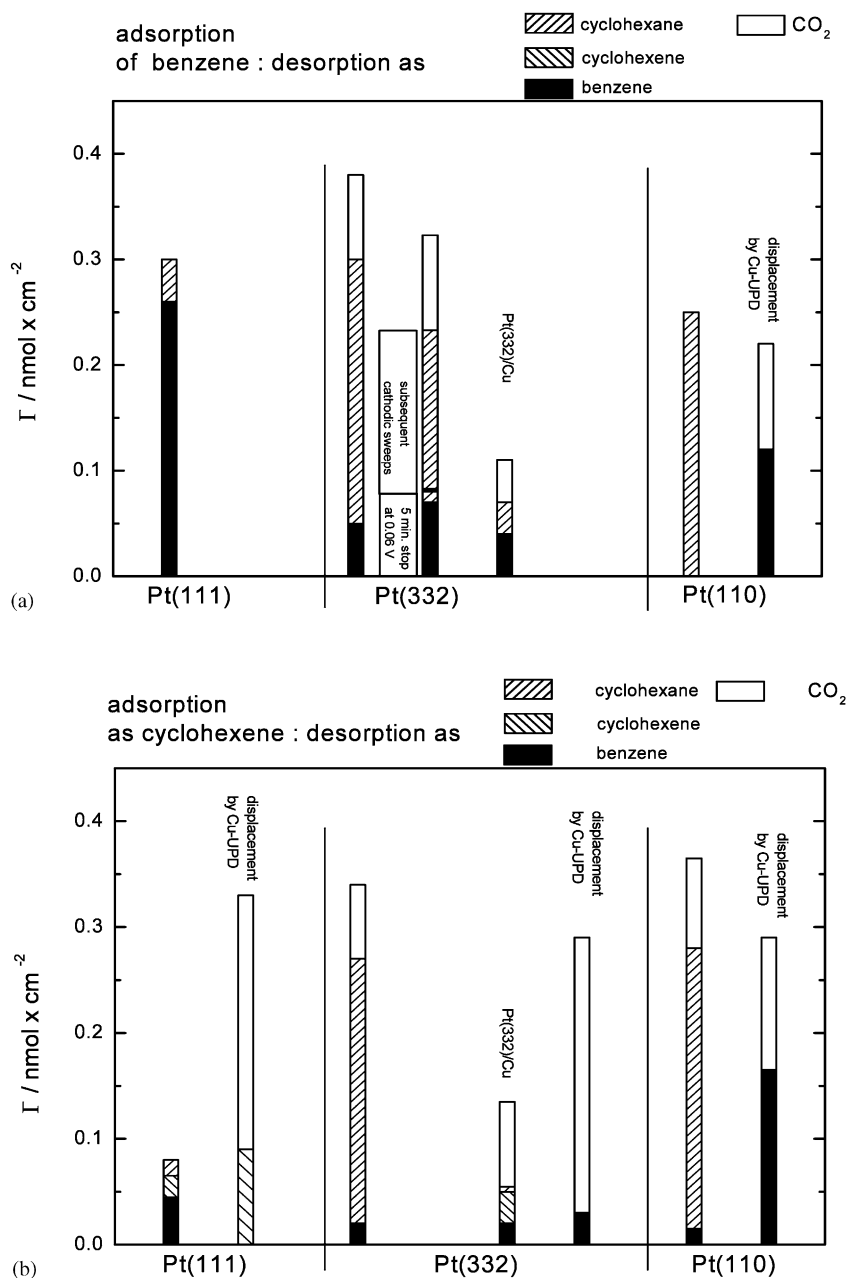
Fig. 8. Absolute amount of species formed from adsorption of benzene (a) and cyclohexene (b) on different platinum surfaces, as detected in potential sweeps in the hydrogen region or by displacement with Cu and during subsequent oxidative potential sweeps (CO_2).

Table 1
Total surface concentration of benzene or cyclohexene adsorbed at Pt(hkl) (calculated from CO_2 evolved during direct oxidation)

Pt(hkl)	$\Gamma_{benzene}$ (nmol $\times$ cm^{-2})	$\Gamma_{cyclohexene}$ (nmol $\times$ cm^{-2})
Pt(111)	0.26 [18]	0.25 [30]
Pt(100)	0.33 [a] [18]	Not measured
Pt(332)	0.36	0.32
Pt(110)	0.34 [18]	0.34 [20]
Ptpc	0.28 [20]	0.28 [31]

[a] From the amount of cathodically desorbed benzene and the CO_2 evolved during subsequent oxidation of the cathodically undesorbable adsorbate.

hydrogenated or not. Alternatively, if the desorption of benzene is slow compared with the potential change during cyclic voltammetry, benzene molecules, which from a thermodynamic point of view could be desorbed as such might only be desorbed when the potential has reached such a low value that hydrogenation is also possible. Since the steps are the catalytic sites, this would require diffusion (on the surface or via solution) to these sites for those benzene molecules, which are adsorbed on the terraces. However, our potential stop (5 min) within the first cathodic sweep during the desorption of adsorbed benzene at Pt(332) at 70 mV (benzene

desorption takes place, but no hydrogenation to cyclo-hexane) shows that the overall ratio between desorbing benzene and cyclohexane is not changed and that the non-hydrogenative desorption of benzene is (nearly) complete at the potential where hydrogenation sets in. Whether an adsorbed benzene molecule is hydrogenated or not, therefore depends on its adsorption site. The hydrogenated molecules might be those which are adsorbed within a certain distance to the steps, i.e. those which are influenced in their adsorption enthalpy (stronger binding) due to the steps. Nevertheless, it is probable that they have to diffuse on the surface to the step sites prior to hydrogenation.

On Pt(111) the small amount of cyclohexane is probably formed at surface defects. Since, according to the above discussion, not only molecules adsorbed at the defect sites are hydrogenated but also those in their vicinity, the relative amount of hydrogenation product at Pt(111) is larger than the relative number of defects.

4.3. Steps as catalytic sites for dehydrogenation

In the case of cyclohexene adsorption at Ptpc and Pt(110) we have shown that cyclohexene is dehydroge-nated to benzene upon adsorption: about 70% of all adsorbed species, either formed after adsorption of benzene or cyclohexene, can be displaced by Cu-UPD solely as benzene [20]. The similarity of the desorption experiments for preadsorbed benzene and cyclohexene indicates that the dehydrogenation also proceeds upon adsorption on the stepped Pt(332). The comparison of the results of the non-reactive displacement of cyclohex-ene adsorbed on Pt(111) and on Pt(332) allow to scrutinize whether the steps are the active sites for the dehydrogenation reaction.

During the non-reactive displacement of cyclohexene adsorbed at Pt(111) by Cu-UPD only cyclohexene can be detected, which amounts to ca. 30% of all adsorbed cyclohexene. Please note that in Fig. 8 the amount of species which was detected is shown. This value corresponds to the amount of displaced species only if the transfer efficiency N was 1. However, a part of the species desorbed during the flow of electrolyte is leaving the cell without being detected, even at very low flow rates; thus, N is decreased to approximately 0.5. Never-theless, the amount of the remaining adsorbate, which is oxidized to CO_2 during the subsequent oxidation after displacement shows that only a small part of the adsorbate can be displaced, much less than for cyclo-hexene adsorbed at Pt(110) or Ptpc, where about 70% of all adsorbed species can be displaced as benzene by Cu-UPD [20]. A reasonable explanation is the following: We already proposed in the past that in the case of cyclohexene adsorbed at Pt(111) besides cyclohexene a further, oxygen containing adsorbate state exists, which could not be detected mass spectrometrically due to its

low vapor pressure and its high solubility in aqueous solution [17], although it is desorbed in the hydrogen region. Furthermore, on Pt(111) this oxygen containing adsorbate amounts to ca. 70%, and is therefore the main adsorbate. Since the total surface concentrations, deter-mined from the direct oxidation and from the oxidation after displacement by Cu-UPD, are more or less equal, a displacement of this adsorbate state can be excluded.

In the case of cyclohexene adsorbed at Pt(332), during the displacement experiments a signal only for benzene was detected, which amounts to ca. 15% of all adsorbed cyclohexene. Due to the uncertainty in the transfer coefficient, this probably means that only between 15 and 30% of the cyclohexene is dehydrogenated upon adsorption and can be displaced as benzene. This is underlined by the observation, that during the direct oxidation of cyclohexene (Fig. 1) only a small preoxida-tion wave is visible, compared with benzene adsorbed at Pt(332) (Fig. 1). The comparison to the Pt(111), how-ever, shows that steps also catalyze the dehydrogenation of cyclohexene to benzene during adsorption. The amount might correspond to cyclohexene adsorbing at step sites. On the other hand, 70–85% of the adsorbate are not detected or possibly stay on the surface. One might expect that this adsorbate corresponds to cyclo-hexene adsorbing on the terraces, and therefore has the same identity as that adsorbed on Pt(111) (probably an oxygen containing adsorbate). Since most of the ad-sorbate desorbs as cyclohexane at potentials in the hydrogen region, the stepped Pt(332) surface is also active for the hydrogenation of this adsorbate state.

The fact that steps are catalytically more active than the atomically smooth surface is well known from the UHV. In the case of hydrogenation reactions, however, the difference does not originate from the easier H–H bond scission at steps, because hydrogen comes from protons. Probably, it is therefore the more stable intermediate formed by addition of a hydrogen which is stabilized at the step site. This is either due to an increased DOS of the d-states close to the Fermi level at the step [38] and/or simply due to a steric effect, which allows also accommodation of a molecule (a transition state) which is not flat.

4.4. Coverage dependence on terrace width

The total surface concentration of adsorbed benzene at the step decorated Pt(332) is much smaller compared with Pt(111) or Pt(332).This is due to the fact, that benzene does not adsorb on Cu; therefore the rows of Cu are a hindrance for an adsorbed adlayer of benzene. The benzene can not adsorb in two rows on a terrace under these conditions, as its illustrated in form of a simple geometric model in Fig. 9. This model takes the STM-study of benzene adsorption on Pt(111) by Itaya and coworkers into account [14]. It should be noted that

Adsorption of benzene

Pt(111)

(a)

Pt(332)
steps decorated
with Cu-UPD

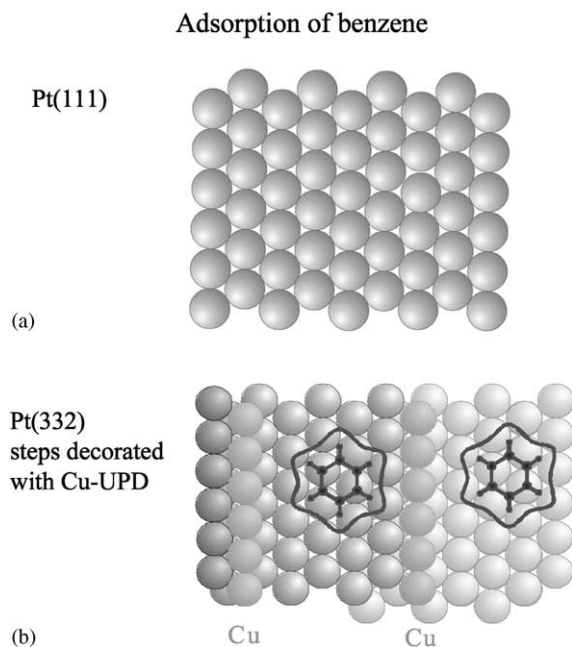(b)   Cu   Cu

Fig. 9. Comparison of the size of a benzene molecule and the $(2\sqrt{3} \times 3)$ unit cell on Pt(111) (a) to the terrace width of a Pt(332) with the steps decorated by Cu-UPD (b).

the annealed single crystal was cooled down in Ar-atmosphere and is probably facetted, at least in part, leading to an increased terrace width and step height and additional presence of kinks [39]. Nevertheless, it is reasonable to assume that areas with large terraces alternate with areas with small terraces, which are not large enough for the adsorption of several rows of benzene molecules.

The effect of Cu may even be enlarged due to the adsorption of sulfate ions, which is stronger on Cu than on Pt. Sulfate is still adsorbed at 0 V versus RHE on Cu(111) [40]. This would prevent the location even of H-atoms of the benzene above the Cu atoms. An electronic effect of Cu leading to a decrease of the adsorption strength also in the vicinity of the Cu atoms can not be excluded at this point.

5. Conclusions

- As in the case of benzene adsorbed on Pt(111) [19], the oxidation of benzene adsorbed on Pt(332) at 0.4 V proceeds in two steps via a partially oxidized adsorbate, possibly benzoquinone. The n_{ox} value of 35 for the complete oxidation (theoretically $n_{ox} = 30$) shows that hardly any other species besides CO_2 is formed as the final oxidation product.
- In the case of cyclohexene adsorbed on Pt(332) at 0.4 V this preoxidation wave is smaller, indicating that

only a part of the adsorbed cyclohexene has been dehydrogenated to adsorbed benzene as confirmed by the Cu displacement experiments, whereas conversion to benzene is complete in the case of Ptpc and Pt(110). Nevertheless, the n_{ox} of 34 shows that CO_2 is also the sole oxidation product.
- The step density of the Pt(332) surface is sufficient for the hydrogenative desorption of adsorbed benzene at negative potentials. The comparison with the adsorption of ethene on Pt(332) suggests that the ratio of the size of the molecule to the terrace width determines the hydrogenation efficiency.
- Also the adsorbate state, which is formed from cyclohexene on the terraces of the stepped surface is hydrogenated at the steps. This adsorbate state most probably has the same identity as that formed on the Pt(111); i.e. is an oxygen containing adsorbate. The step sites also catalyze the dehydrogenation of cyclohexene to benzene upon adsorption, as can be deduced from the displacement (by Cu-UPD) experiments of cyclohexene adsorbed at 0.35 V on Pt(111) and Pt(332). However, the step density is not sufficient for complete dehydrogenation of all adsorbing molecules, since the preoxidation wave in the CV curve (during the direct oxidation) is smaller compared with the case of adsorbed benzene and since the displacement by Cu is rather incomplete.
- The step sites are the active sites for the hydrogenation reactions, as blocking of them by inactive Cu (nearly) completely suppresses the hydrogenative formation of cyclohexane. The adsorption site, e.g. the distance from a step, determines whether an adsorbed molecule is hydrogenated or not. The desorption of benzene molecules as such is (nearly) complete at the potential where hydrogenation sets in.
- Step decoration of the Pt(332) leads to a decrease of the total surface concentration of adsorbed benzene by a factor of ca. 2. A possible origin is that benzene can not adsorb in two parallel rows on a terrace any longer since benzene does not adsorb on Cu. The rows of Cu adsorbed at the step sites, therefore, are a hindrance for an adsorbed adlayer of benzene.

References

[1] G. Somorjai, Chemistry in Two Dimensions: Surfaces, Cornell University Press, Ithaka and London, 1981.

[2] S. Davis, G. Somorjai, in: D. King, D. Woodruff (Eds.), The Chemical Physics of Solid Surfaces and Heterogenous Catalysis. Fundamental Studies of Heterogenous Catalysis, vol. 4, Elsevier Verlag, 1982, p. 217ff.

[3] F. Zaera, Chem. Rev. 95 (1995) 2651.

[4] N. Sheppard, C. LaCruz, Advances in Catalysis, vol. 42, 1998, p. 181ff.

[5] M. Tsai, E.L. Muetterties, J. Am. Chem. Soc. 104 (1982) 2534.

[6] M. Tsai, E.L. Muetterties, J. Am. Chem. Soc. 104 (1982) 2539.

[7] W. Manner, G. Girolami, R. Nuzzo, J. Phys. Chem. B 102 (1998) 10295.

[8] X.C. Su, K. Kung, J. Lahtinen, R.Y. Shen, G.A. Somorjai, Catal. Lett. 54 (1998) 9.

[9] M.E. Pansoy-Hjelvik, P. Schnabel, J.C. Hemminger, J. Phys. Chem. B 104 (2000) 6554.

[10] K.R. McCrea, G.A. Somorjai, J. Mol. Catal. A-Chem. 163 (2000) 43.

[11] P. Zebisch, M. Stichler, P. Trischberger, M. Weinelt, H. Steinrück, Surf. Sci. 396 (1998) 161.

[12] F. Thomas, N. Chen, I. Lee, L. Ford, P. Blowers, R.I. Masel, J. Vacuum Sci. Technol. A-Vacuum Surf. Films 17 (1999) 2339.

[13] F.S. Thomas, N.S. Chen, L.P. Ford, R.I. Masel, Surf. Sci. 486 (2001) 1.

[14] M. Saeys, M.F. Reyniers, G.B. Marin, M. Neurock, J. Phys. Chem. B 106 (2002) 7489.

[15] S.-L. Yau, Y.-G. Kim, K. Itaya, in: A. Wieckowski, K. Itaya (Eds.), Sixth International Symposium on Electrode Processes, vols. 96-8, Electrochemical Society, Los Angeles, 1996, p. 243.

[16] X.-Y. Xiao, Ph.D. thesis, Bonn University, Bonn, 2002.

[17] H. Baltruschat, in: A. Wieckowski (Ed.), Interfacial Electrochemistry, Marcel Dekker, New York, Basel, 1999, p. 577.

[18] U. Schmiemann, H. Baltruschat, J. Electroanal. Chem. 347 (1993) 93.

[19] T. Hartung, U. Schmiemann, I. Kamphausen, H. Baltruschat, Anal. Chem. 63 (1991) 44.

[20] U. Müller, H. Baltruschat, J. Phys. Chem. B 104 (2000) 5762.

[21] U. Müller, A. Stoyanova, H. Baltruschat, in: A. Wieckowski, K. Itaya (Eds.), Sixth International Symposium on Electrode Processes, Meeting of the Electrochemical Society, vols. 96-8, Electrochemical Society, Los Angeles, 1996, p. 257.

[22] T. Löffler, X. Xiao, H. Baltruschat, J. Electroanal. Chem. (2003), submitted for publication

[23] P. Berenz, S. Tillmann, H. Massong, H. Baltruschat, Electrochim. Acta 43 (1998) 3035.

[24] H. Massong, H.S. Wang, G. Samjeske, H. Baltruschat, Electrochim. Acta 46 (2000) 701.

[25] G. Samjeské, X.-Y. Xiao, H. Baltruschat, Langmuir 18 (2002) 4659.

[26] M. Macia, E. Herrero, M. Feliu, A. Aldaz, Electrochem. Commun. 1 (1999) 87.

[27] O. Wolter, J. Heitbaum, Ber. Bunsenges. Phys. Chem. 88 (1984) 2.

[28] U. Müller, U. Schmiemann, A. Dülberg, H. Baltruschat, Surf. Sci. 335 (1995) 333.

[29] U. Schmiemann, Z. Jusys, H. Baltruschat, Electrochim. Acta 39 (1994) 561.

[30] U. Schmiemann, U. Müller, H. Baltruschat, Electrochim. Acta 40 (1995) 99.

[31] U. Müller, Thesis, Witten-Herdecke, Witten-Herdecke, 1996.

[32] J. Clavilier, K.E. Achi, A. Rodes, J. Electroanal. Chem. 272 (1989) 253.

[33] T. Hartung, H. Baltruschat, Langmuir 6 (1990) 953.

[34] N. Furuya, S. Koide, Surf. Sci. 220 (1989) 18.

[35] H. Baltruschat, U. Schmiemann, Ber. Bunsenges. Phys. Chem. 97 (1993) 452.

[36] J.L. Rodriguez, E. Pastor, Electrochim. Acta 45 (2000) 4279.

[37] R. Bussar, Diploma thesis, Bonn University, Bonn, 2002.

[38] B. Hammer, O.H. Nielsen, J.K. Norskov, Catal. Lett. 46 (1997) 31.

[39] E. Herrero, J.M. Orts, A. Aldaz, J.M. Feliu, Surf. Sci. 440 (1999) 259.

[40] M. Lennartz, P. Broekmann, M. Arenz, C. Stuhlmann, K. Wandelt, Surf. Sci. 442 (1999) 215.